Dalton Transactions

Accepted Manuscript

ROYAL SOCIETY OF CHEMISTRY

www.rsc.org/dalton

Cite this: DOI: 10.1039/c0xx00000x

www.rsc.org/xxxxxx

ARTICLE TYPE

Ethylene polymerization by the thermally unique 1-[2-(bis(4-fluoro phenyl)methyl)-4,6-dimethylphenylimino]-2-aryliminoacenaphthylnickel precursors

Shizhen Du,[a] Qifeng Xing,[a] Zygmunt Flisak,[a] Erlin Yue,[a] Yang Sun,[a] and Wen-Hua Sun*[a,b]

Received (in XXX, XXX) Xth XXXXXXXXX 20XX, Accepted Xth XXXXXXXXX 20XX
DOI: 10.1039/b000000x

A series of 1-[2-(bis(4-fluorophenyl)methyl)-4,6-dimethylphenylimino]-2-aryliminoacenaphthylene derivatives together with the corresponding nickel bromide complexes was synthesized and characterized. Representative complexes **C2** and **C5** were characterized by the single-crystal X-ray diffraction, revealing a distorted tetrahedral geometry. Upon activation with either methylaluminoxane (MAO) or ethylaluminum sesquichloride (EASC), all nickel complexes exhibited high activities towards ethylene polymerization, producing polyethylene with relatively low degree of branching and narrow polydispersity. Complex **C1** maintained good activity at elevated reaction temperature, which indicates significant thermal stability of the active species.

Introduction

During the past two decades, the development of highly active late-transition-metal complex pre-catalysts has received increasing attention both from academia and industry.[1] The pioneering works by Brookhart and co-workers[2a,2b] dealt with the nickel- and palladium-based α-diimine complex pre-catalysts, producing high-molecular-weight polyethylenes with various polymer architectures, ranging from linear to hyperbranched. Though Brookhart-type catalysts exhibit high activity and produce polyethylenes of various properties, they are usually limited by relatively poor thermal stability. Considering the highly exothermic process of ethylene polymerization, the critical factor in the industrial application is to maintain good activity within the operational temperature of around 80ºC.[3] To solve this problem, various efforts have been made to improve the thermal stability of α-diimine-based catalytic systems, e.g. modification of substituents.[4] Recently, benzhydryl-derived ligands have attracted significant attention due to the inhibition of N-aryl rotations by steric interactions; this can protect the active species and enhance the thermal stability of the catalyst.[5] In our previous works, series of nickel complex pre-catalysts bearing benzhydryl-derived ligands including 1,2-bis(arylimino)acenaphthylenes,[6] 2-(aryliminomethyl)pyridines[7] and 2,3-bis(arylimino)butane derivatives[5g,8] showed high catalytic activities together with enhanced thermal stability. Application of 2,6-dibenzhydryl-4-methylbenzenamine as a bulky moiety represents the progress in 1,2-bis(arylimino)acenaphthylylnickel pre-catalysts for ethylene polymerization,[6a,6b,6f] where sterically demanding ligands enhance the thermal stability of the catalytic system, simultaneously lowering the catalytic activity.[6f] Introduction of 2,6-dibenzhydryl-4-chlorobenzenamine[6c] and 2,6-bis(bis(4-fluorophenyl)methyl)-4-methylbenzenamine[6e] further improves the catalytic activities of the corresponding nickel complexes. Meanwhile the computational work indicates that the catalytic activities of the nickel-based catalysts improve when the electronegativity of the ligand is increased.[9] Encouraged by these results, we prepared 2-[bis(4-fluorophenyl)methyl]-4,6-dimethylbenzenamine and used it to synthesize acenaphthylene-1-[2-(bis(4-fluorophenyl) methyl)-4,6-dimethylphenylimino]-2-arylimine derivatives and the corresponding nickel complexes for ethylene polymerization. Details regarding the catalytic activity and thermal stability of the title complexes, thereof **C1-C6**, will be presented in this paper.

Results and discussions

Synthesis and Characterization of the Organic Compounds (L1-L6) and Nickel Complexes (C1-C6).

The stoichiometric reaction of acenaphthylene-1,2-dione with 2-[bis(4-fluorophenyl)methyl]-4,6-dimethylbenzenamine in the mixture of dichloromethane and ethanol at room temperature affords the minor 1,2-bis[2-(bis(4-fluorophenyl)methyl)-4,6-dimethylphenylimino]acenaphthylene (**L1**) and major 2-[2-(bis(4-fluorophenyl)methyl)-4,6-dimethylphenylimino]acenaphthylen-1-one, which further condensed with various anilines forms 1-[2-(bis(4-fluorophenyl)methyl)-4,6-dimethylphenylimino]-2-aryl-iminoacenaphthylene derivatives (**L2-L6**). The bis(imino) acenaphthylene compounds (**L1-L6**) react individually with an equivalent of (DME)$NiBr_2$ in dichloromethane to produce the corresponding nickel bromide complexes (**C1–C6**) in good yields. The synthesis of organic compounds (**L1-L6**) and the corresponding nickel complexes (**C1-C6**) is summarized in Scheme **1**.

All the organic compounds were characterized and identified by the FT-IR spectra, NMR measurements as well as elemental

analyses, and the identities of diiminonickel bromide complexes (**C1-C6**) was confirmed by FT-IR spectroscopy and elemental analysis. Comparing the FT-IR spectra of the nickel complexes (**C1-C6**) with the corresponding ligands (**L1-L6**), we found that the $\upsilon_{(C=N)}$ stretching vibration of **L1-L6** (1670 and 1640 cm^{-1}) shifts to 1650 and 1620 cm^{-1} in the nickel complexes, reflecting the effective coordination between the nickel ion and the N_{imino} atom. Furthermore, the single crystals of representative complexes **C2** and **C5** were obtained and submitted for the X-ray crystallographic study to confirm their structure in the solid state.

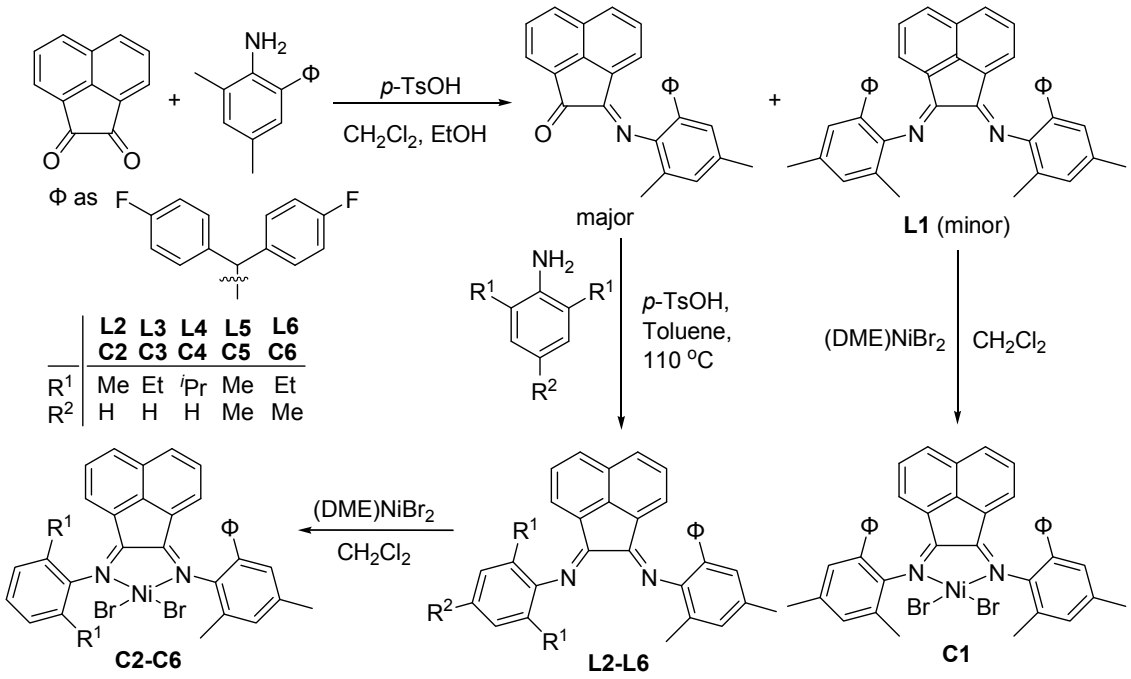

Scheme 1. Synthetic procedure for compounds **L1-L6** and **C1-C6.**

X-ray Crystallographic Study.

Crystals of **C2** and **C5** suitable for the single crystal X-ray diffraction study were obtained by the slow diffusion of diethyl ether into the respective dichloromethane solutions. The molecular structures are shown in Figs. **1** and **2** and the selected bond lengths and angles are listed in Table **1**. The complexes **C2** and **C5** exhibit distorted tetrahedral geometry around the nickel center, in which the N1, N2 and Br2 atoms form the plane with the Br1 atom occupying the apical position. In **C2**, the nickel atom is located outside of the plane by 0.808 Å along with the N1-Ni1-N2 angle of 82.98(18)° and the Ni1-N1 and Ni1-N2 bond lengths of 2.024(4) Å and 2.022(5) Å, respectively. Typically for the C=N double-bond, the N1-C11 and N2-C12 distances are much shorter than N1-C21 and N2-C13: 1.283(7) Å and 1.278(7) Å vs. 1.431(7) Å and 1.447(7) Å, respectively. The coordination plane containing N1, N2 and Ni1 is almost perpendicular to both N-aryl rings with the dihedral angles of 82.61° and 69.06°, respectively. Similar to the case of **C2**, the central nickel atom in **C5** is 0.918 Å away from the plane along with the N1-Ni1-N2 angle of 83.33(18)° and the Ni1-N1 and Ni1-N2 bond lengths of 2.038(5)Å and 2.023(4) Å, respectively. The N1-C11 and the N2-C12 bonds of 1.286(7) Å and 1.298(6) Å are also typical for the imino group and shorter than the N1-C22 and N2-C13 single bonds (1.438(7) Å and 1.437(7) Å, respectively). The plane composed by N1, N2, and Ni1 forms the dihedral angle of 77.16° with the N1-aryl ring and 68.49° with the N2-aryl ring, respectively.

Table 1. Selected bond lengths (Å) and angles (°) for **C2** and **C5**.

	C2	**C5**
	Distance / Å	
Ni(1)-N(1)	2.024(4)	2.038(5)
Ni(1)-N(2)	2.022(5)	2.023(4)
Ni(1)-Br(1)	2.3490(11)	2.3458(10)
Ni(1)-Br(2)	2.3285(10)	2.3352(11)
N(1)-C(11)	1.283(7)	1.286(7)
N(2)-C(12)	1.278(7)	1.298(6)
N(2)-C(13)	1.447(7)	1.437(7)
N(1)-C(21)	1.431(7)	
N(1)-C(22)		1.438(7)
	Bond angles / °	
N(1)-Ni(1)-N(2)	82.98(18)	83.33(18)
N(1)-Ni(1)-Br(2)	107.31(13)	102.29(13)
N(2)-Ni(1)-Br(2)	125.60(13)	119.70(13)
N(1)-Ni(1)-Br(1)	111.58(12)	116.72(13)
N(2)-Ni(1)-Br(1)	100.48(13)	103.68(13)
Br(1)-Ni(1)-Br(2)	122.18(4)	124.26(4)

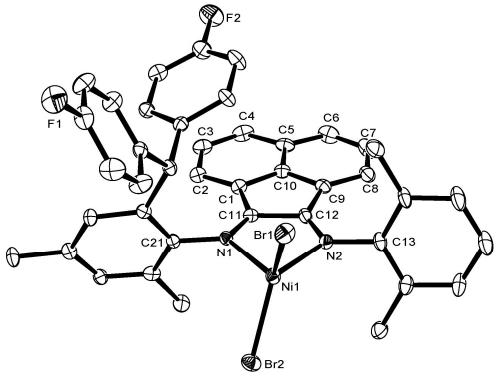

Figure 1. ORTEP drawing of **C2**. Thermal ellipsoids are shown at the 30% probability level. Hydrogen atoms have been omitted for clarity.

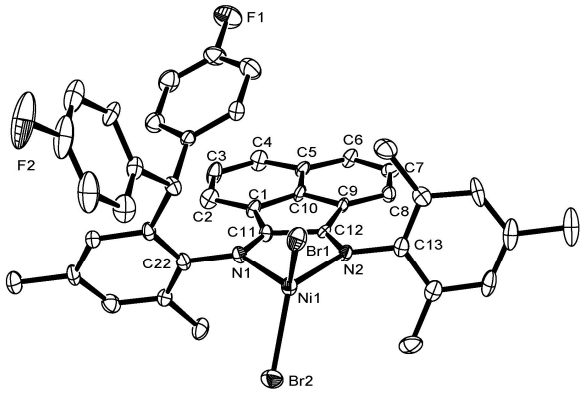

Figure 2. ORTEP drawing of **C5**. Thermal ellipsoids are shown at the 30% probability level. Hydrogen atoms have been omitted for clarity.

Ethylene Polymerization.

Various alkylaluminium reagents as co-catalysts were used to evaluate the catalytic activity in ethylene polymerization under 10 atm at ambient temperature. The results of polymerization tests are collected in Table **2**. Upon activation with MAO, Et_2AlCl and EASC, the pre-catalyst **C5** exhibited high activity of up to 10^6 g of PE (mol of Ni)$^{-1}$ h^{-1} in ethylene polymerization. For further detailed investigation of the catalytic properties, both MAO and EASC were selected as co-catalysts.

Table 2. Ethylene polymerization by complex **C5** with various co-catalysts [a]

Entry	Co-cat	Al/Ni	Act [b]	M_w [c]	*Mw/Mn* [c]	T_m [d] (ºC)
1	MAO	1000	3.41	3.7	2.8	126.3
2	MMAO	1000	0.83	6.0	2.0	126.1
3	Et_2AlCl	200	3.07	3.8	3.0	105.9
4	EASC	200	4.97	1.8	2.2	102.8
7	Me_2AlCl	200	trace			

[a]Conditions: 2.0 μmol Ni, 100 mL toluene, 10 atm ethylene, T = 30 ºC, t = 30 min. [b]10^6 g of PE (mol of Ni)$^{-1}$ h^{-1}. [c]Determined by GPC, and M_w: 10^5 g mol^{-1}. [d]Determined by DSC.

Ethylene polymerization with the C1-C6/MAO system.

The optimum conditions for the pre-catalyst **C5**, such as the molar ratio of Al/Ni, time and temperature, were evaluated in the presence of MAO, and the results are collected in Table **3**. On increasing the Al/Ni molar ratio from 1000 to 4000 (entries 1 – 6, Table **3**) at a fixed temperature of 30ºC and the reaction time of 30 min, the best activity of 7.20 × 10^6 g of PE (mol of Ni)$^{-1}$ h^{-1} was achieved for a value of 2500 (entry 4, Table **3**). The catalytic behaviors of **C5**/MAO system at different temperatures were further investigated at this particular Al/Ni molar ratio. For the temperature varied from 20ºC to 80ºC (entries 4 and 7 – 11, Table **3**), the optimum activity was observed at 30ºC. Higher temperatures led to a marked decrease in activity down to 0.63 × 10^6 g of PE (mol of Ni)$^{-1}$ h^{-1}, which is consistent with the previous reports on α-diimine nickel complexes.[6,8,10] For different reaction times ranging from 5 min to 60 min (entries 4, 12 – 14, Table **3**), the highest activity was observed within 5 minutes (entry 12, Table **3**) and then the activity decreased, which suggests that the active species are formed quickly after adding MAO and undergo gradual deactivation along with the reaction time. Regarding ethylene pressure, the ethylene polymerization was conducted under the different pressures of 1 atm, 5 atm and 10 atm (entries 4, 15 and 16, Table **3**); higher activities were achieved for higher ethylene pressures. With the optimum catalytic conditions fixed (the Al/Ni ratio of 2500, temperature of 30ºC and polymerization time of 30 min), other analogs were investigated for ethylene polymerization (entries 17 – 21, Table **3**) with good activities in all cases. Accordingly (entries 4 and 18 – 21, Table 3), the activity decreases in the order as **C2** [2,4-di(Me)] > **C3** [2,6-di(Et)] > **C4** [2,6-di(i-Pr)], and **C5** [2,4,6-tri(Me)] > **C6** [2,6-di(Et)-4-Me], consistent with the observation[6c,6g] as well as computationally higher activity with electronegative ligand.[9] It was observed that **C1** and **C4** showed lower activities than other complexes, which indicates that the bulky substituents attached to the phenyl ring at the *ortho*-positions within the ligands hinder the ethylene insertion into the Ni-C bond and this results in a lower polymerization rate.[3b,6b,6d] Additionally, the polyethylene obtained with **C1** at 30ºC exhibits high molecular weight of 1.0 × 10^6 g mol^{-1} with narrow polydispersity (entry 17, Table **3**).

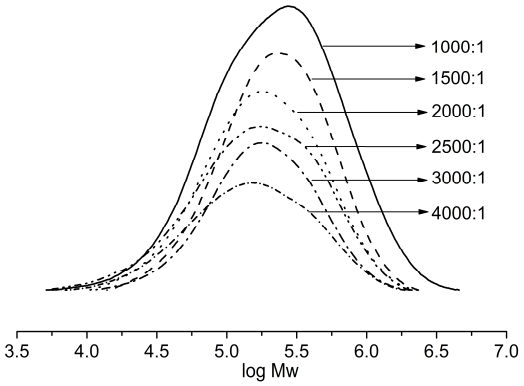

Figure 3. GPC curves for the polyethylenes by C5/MAO system with various Al/Ni ratios (entries 1 – 6, Table 3).

Considering the application potential of the polyethylenes obtained, we were also concerned about their properties. On increasing the Al/Ni molar ratio for the **C5**/MAO system, polyethylenes of lower molecular weights were produced with the slight changes in polydispersity (entries 1 – 6, Table **3**), which indicates that the higher molar ratios of Al/Ni enhance the possibility of chain transfer from the active nickel species to the

aluminium species, which is one of the termination reactions.[10b,10c] The appropriate GPC curves are shown in Fig. **3**.

Reaction temperature also greatly affected the molecular weights of polyethylenes obtained. Along with elevating polymerization temperature from 20ºC to 80ºC (entries 4 and 7 – 11, Table **3**), a gradual decrease in activity as well as in the molecular weight was observed, which was consistent with the findings reported previously for the α-diimine nickel catalytic systems.[6,8,10] The GPC curves (Fig. **4**) clearly show that the molecular weight decreases with the temperature, but it increases slightly for longer reaction periods (Fig. **5)**.

Table 3. The catalytic properties of complexes **C1-C6** activated with MAO [a]

Entry	Pre-catalyst	T/ºC	t/min	Al/Ni	Act [b]	M_w [c]	Mw/Mn [c]	T_m [d] (ºC)
1	**C5**	30	30	1000	3.41	3.7	2.8	126.3
2	**C5**	30	30	1500	4.34	3.1	2.1	115.9
3	**C5**	30	30	2000	6.12	2.7	2.3	114.2
4	**C5**	30	30	2500	7.20	2.6	2.7	111.8
5	**C5**	30	30	3000	4.92	2.5	2.0	119.1
6	**C5**	30	30	4000	3.03	2.3	2.5	107.5
7	**C5**	20	30	2500	5.12	3.8	2.4	118.1
8	**C5**	40	30	2500	5.93	1.0	1.9	92.1
9	**C5**	50	30	2500	3.92	0.9	1.9	77.3
10	**C5**	60	30	2500	2.28	0.8	2.0	72.7
11	**C5**	80	30	2500	0.63	0.5	2.0	63.7
12	**C5**	30	5	2500	13.6	2.0	2.1	101.8
13	**C5**	30	15	2500	9.90	2.3	2.0	103.1
14	**C5**	30	60	2500	4.88	3.1	2.0	117.0
15[e]	**C5**	30	30	2500	trace			
16[f]	**C5**	30	30	2500	2.13	2.5	2.3	108.8
17	**C1**	30	30	2500	5.03	10	2.1	116.8
18	**C2**	30	30	2500	6.27	2.4	2.2	91.4
19	**C3**	30	30	2500	5.58	4.3	1.9	112.2
20	**C4**	30	30	2500	5.20	4.6	2.1	117.1
21	**C6**	30	30	2500	5.31	8.5	2.2	122.3

[a]Conditions: 2.0 μmol of Ni; 100 mL toluene for 10 atm ethylene. [b]10^6 g of PE (mol of Ni)$^{-1}$ h^{-1}.
[c]M_w: 10^5 g mol^{-1}, M_w and M_w/M_n determined by GPC. [d]Determined by DSC. [e]1 atm. [f]5 atm.

Figure 4. GPC curves for the polyethylenes obtained by **C5**/MAO system at different temperatures (entries 4, 7 – 11, Table **3**).

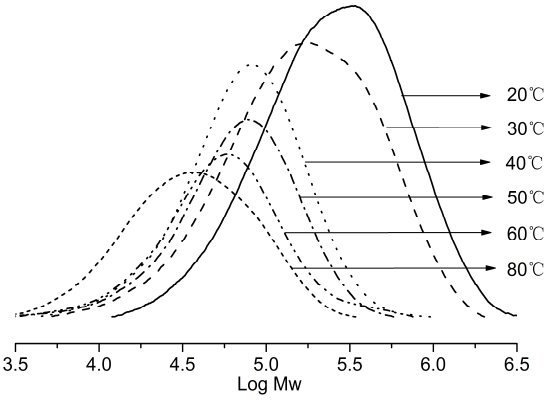

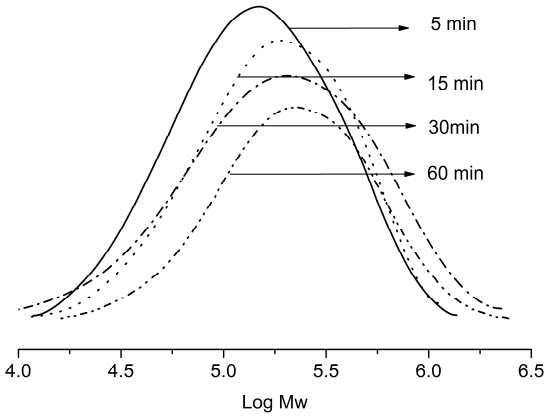

Figure 5. GPC curves for the polyethylenes obtained by **C5**/MAO system at different reaction time (entries 4, 12 – 14, in Table **3**).

According to the DSC experiment, the majority of T_m values for polyethylenes obtained were higher than 100ºC, which confirms high molecular weights and suggests low degree of branching. Polyethylene obtained at 30ºC was characterized by the high-temperature ^{13}C NMR spectroscopy (Fig. **6**). Being interpreted according to the literature,[11] 27 branches in 1000 carbons were measured including methyl (63.26%), ethyl (20.41%) and longer chains (16.33%).

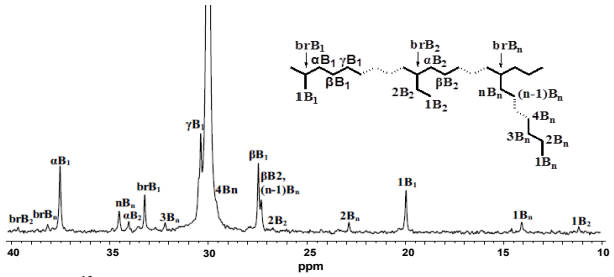

Figure 6.^{13}C NMR spectrum of the polyethylene by **C5**/MAO at 30ºC (entry 4, in Table 3).

Table 4. The catalytic properties of complexes **C1-C6** activated with EASC [a]

Entry	Pre-catalyst	T/ºC	t/min	Al/Ni	Act [b]	M_w [c]	*Mw/Mn* [c]	T_m [d] (ºC)
1	**C5**	30	30	200	4.97	1.8	2.2	102.8
2	**C5**	30	30	300	5.28	1.8	2.1	108.8
3	**C5**	30	30	400	5.92	1.9	2.2	109.4
4	**C5**	30	30	500	5.23	1.9	2.1	102.8
5	**C5**	30	30	600	3.55	2.2	2.2	107.6
6	**C5**	30	30	700	2.77	2.7	2.2	106.0
7	**C5**	20	30	400	8.11	3.5	2.6	120.3
8	**C5**	40	30	400	5.26	1.0	1.7	78.8
9	**C5**	50	30	400	5.07	0.8	1.7	70.3
10	**C5**	60	30	400	3.40	0.6	1.7	68.7
11	**C5**	80	30	400	0.60	0.3	1.8	59.4
12	**C5**	20	5	400	12.6	2.3	2.2	121.9
13	**C5**	20	15	400	9.14	3.0	2.4	121.2
14	**C5**	20	60	400	5.20	4.2	2.0	119.3
15[e]	**C5**	20	30	400	trace			
16[f]	**C5**	20	30	400	2.27	2.8	2.4	110.6
17	**C1**	20	30	400	4.50	7.1	1.9	116.7
18	**C2**	20	30	400	6.71	5.6	2.0	123.7
19	**C3**	20	30	400	5.56	7.0	1.9	117.1
20	**C4**	20	30	400	5.48	4.5	2.1	112.4
21	**C6**	20	30	400	5.99	5.2	2.0	113.2

[a]Conditions: 2.0 μmol of Ni; 100 mL toluene for 10 atm ethylene. [b]10^6 g of PE (mol of Ni)$^{-1}$ h^{-1}.
[c]M_w: 10^5 g mol^{-1}, M_w and M_w/M_n determined by GPC. [d]Determined by DSC. [e]1 atm. [f]1 atm.

Ethylene polymerization with C1-C6/EASC system.

Cite this: DOI: 10.1039/c0xx00000x

www.rsc.org/xxxxxx

ARTICLE TYPE

In a similar manner, now using EASC as co-catalyst, the pre-catalyst **C5** was again investigated for the optimum polymerization parameters including the Al/Ni molar ratio, reaction time and temperature; the results are shown in Table **4**. The **C1**-**C6**/EASC systems also exhibit high activity in ethylene polymerization, affording polyethylenes with high molecular weight and narrow polydispersity. Adopting various Al/Ni molar ratios, higher catalytic activities were observed on increasing the Al/Ni molar ratio from 200 to 400 (entries 1 – 3 in Table **4**), and the best activity was observed for the Al/Ni molar ratio of 400 (5.92×10^6 g of PE (mol of Ni)$^{-1}$ h^{-1}). On further increasing the Al/Ni molar ratio (entries 4 – 6 in Table **4**), a slight decrease in the catalytic activity was observed. In addition, the polyethylenes obtained with different EASC amounts exhibited slight variation in polydispersity. Interestingly, the catalytic system with higher Al/Ni molar ratios produced polyethylenes with higher molecular weights (Fig. **7**), unlike the majority of catalytic systems based on late-transition metal complex pre-catalysts. We speculate that this abnormality may be ascribed to the large encumberment effect: with larger amounts of the co-catalyst, the active species are stabilized, and chain propagations surpass both chain migrations and termination. As opposed to the **C1**-**C6**/MAO catalytic systems, the **C1**-**C6**/EASC system performs with the best activity at 20ºC (entry 7 in Table **4**). When the temperature is elevated from 20ºC to 80ºC, the catalytic activity decreases rapidly from 8.11×10^6 g of PE (mol of Ni)$^{-1}$ h^{-1} down to 0.60×10^6 g of PE (mol of Ni)$^{-1}$ h^{-1} (entries 3, 7 – 11 in Table **4**). Regarding the polyethylenes obtained, the higher molecular weights were achieved at the lower reaction temperatures (Fig. **8**). Moreover, on further prolonging the reaction time (entries 3, 12 – 14, in Table **4**), the activity of the system gradually decreased, probably due to the decay of active species. Meanwhile, the molecular weights of obtained polyethylenes increased slightly in longer reaction period. The results of GPC measurements are shown in Fig. **9**. The representative polyethylene obtained at 30ºC was also characterized by high-temperature ^{13}C NMR spectroscopy (Fig. **10**), and the results indicate 43 branches per 1000 carbons with methyl (65.28%), ethyl (3.99%) and longer chains (30.73%).

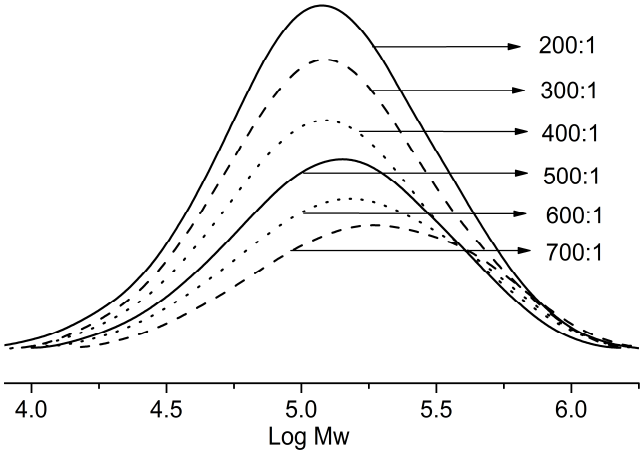

Figure 7. GPC curves for the polyethylenes by the **C5**/EASC system with various Al/Ni ratios (entries 1 – 6, Table 4).

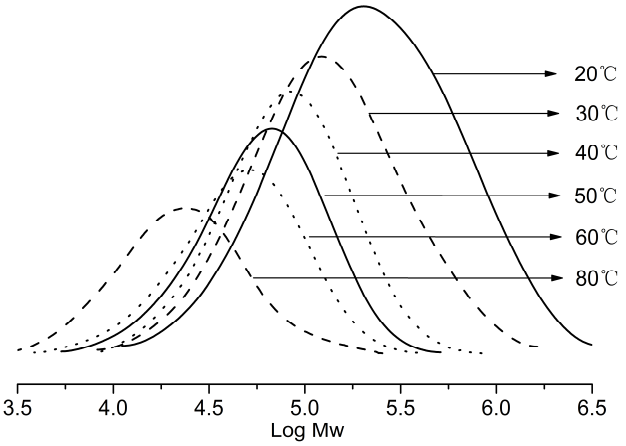

Figure 8. GPC curves for the polyethylenes obtained by the **C5**/EASC system at different temperatures (entries 3, 7 – 11, Table 4).

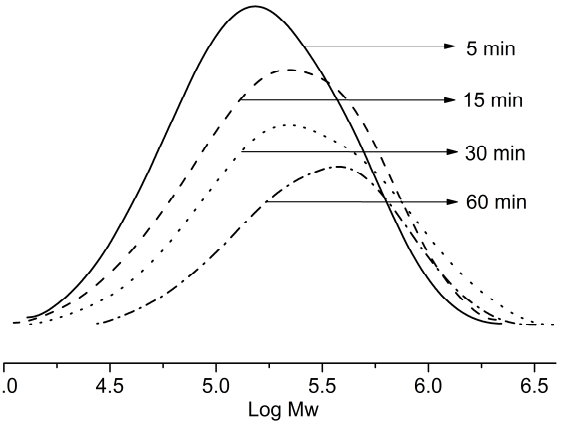

Figure 9. GPC curves for the polyethylenes obtained by the **C5**/EASC system at different reaction time (entries 3, 12 – 14, in Table 4).

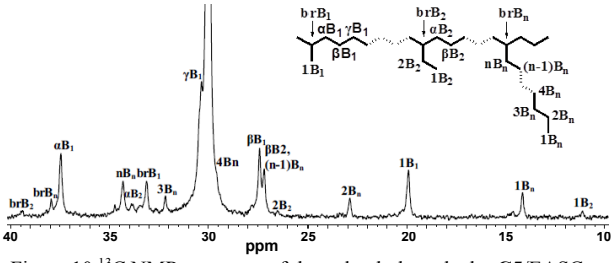

Figure 10.[13]C NMR spectrum of the polyethylene the by **C5**/EASC at 30ºC (entry 3, in Table 4).

Employing the optimum conditions (the Al/Ni molar ratio of 400, the temperature of 20ºC and the reaction time of 30 min), all the other pre-catalysts were screened (entries 3, 17 – 21, in Table **4**). For all the catalytic systems, the presence of the single-site active species was conspicuous and polyethylenes with molecular weight of up to 10^5 g mol^{-1} as well as narrow polydispersity were produced. Similarly, the systems based on **C1** and **C4** with the bulky substituents attached to the phenyl ring at the *ortho*-position within the ligands exhibited lower activity than the other analogs, which is consistent with the activity trend observed for the catalytic systems activated with MAO. Pre-catalyst **C1** afforded polyethylene with the highest molecular weight (7.1 × 10^5 g mol^{-1}) among all **C1**-**C6**/EASC systems.

Pre-catalyst **C1** was then screened for ethylene polymerization at elevated temperature (60ºC – 80ºC) and the results are collected in Table **5**. Upon activation with different co-catalysts, pre-catalyst **C1** exhibits outstanding activities of up to 10^6 g·mol^{-1}(Ni)·h^{-1} as well as narrow polydispersity of the resulting polyethylenes. The **C1**/EASC system shows especially good thermal stability at elevated temperature (80ºC), and modest activity of 3.48 × 10^6 g of PE (mol of Ni)$^{-1}$ h^{-1} was observed (entry 6, Table **5**). The lower activities at higher temperatures were observed mainly due to both deactivation of the active species and the lower solubility of ethylene in toluene at elevated temperatures; therefore we also report the adjusted activities obtained through calculating the ethylene concentrations at different temperatures ($C_{ethylene}$, mol L^{-1} atm^{-1}, Table **5**),[12] indicating better activities observed at elevated temperature ranging from 60ºC to 80ºC. The adjusted activities suggest that ethylene solubility in toluene is a key factor affecting the catalytic activity.

It should be mentioned that the bulky benzhydryl substituents on the aryl rings might have a dual role in the catalyst.[4a] First, they protect the axial positions of the metal center against the monomer access and thus limit potential termination reactions.[2a,2c] Second, they also prohibit free rotation of the phenyl ring around the C-N bond, which would otherwise lead to the formation of agostic interactions between the nickel center and the hydrogen atoms within the ligand and – as a consequence – deactivation of the catalyst.[2d] We would like to emphasize that the introduction of only one benzhydryl substituent into the ligand by using unsymmetrically substituted anilines in the synthetic procedure reported by us earlier[6a,8a] and further refined within the current work (see Scheme **1**) is sufficient to achieve satisfactory thermostability of the catalyst without any marked loss in its activity. On the contrary, recently reported systems containing symmetrical 2,6-bis(benzhydryl)-4-methylphenyl moieties[5g,6f] – although exceptionally thermostable – do not attain impressively high activities at any temperature comparing with those incorporating unsymmetrically substituted aryl rings.[6a,8a] Therefore the current work represents further progress in the design of the highly active systems of moderate thermostability.

Table 5. Ethylene polymerization by pre-catalyst **C1** [a] at elevated temperature.

Entry	Co-catalyst	T/ºC	t/min	Al/Ni	Act [b]	Adjusted-Act [c]	M_w [d]	*Mw/Mn* [d]	T_m [e] (ºC)
1	MAO	60	30	2500	3.55	4.14	2.2	1.8	60.7
2	MAO	70	30	2500	3.07	4.02	1.5	2.0	57.8
3	MAO	80	30	2500	0.92	1.34	1.3	1.8	53.4
4	EASC	60	30	400	4.93	5.75	1.8	2.4	64.3
5	EASC	70	30	400	3.82	5.01	1.4	2.2	44.7
6	EASC	80	30	400	3.48	5.06	0.9	2.0	42.5

[a]Conditions: 2.0 μmol Ni, 100 mL toluene, 10 atm ethylene. [b]10^6 g of PE (mol of Ni)$^{-1}$ h^{-1}. [c]10^6 g of PE (mol of Ni)$^{-1}$ h^{-1} $C_{ethylene}^{-1}$. [d]Determined by GPC, and M_w: 10^5 g mol^{-1}. [e]Determined by DSC.

Conclusions

The synthesis and characterization of nickel based ethylene polymerization pre-catalysts bearing acenaphthylene-1-[2-(bis(4-fluorophenyl)methyl)-4,6-dimethylphenylimino]-2-arylimine derivatives was carried out. Upon activation with various co-catalysts, such as MAO and EASC, all pre-catalysts achieved outstanding catalytic activity for ethylene polymerization with activities of up to 10^6 g of PE (mol of Ni)$^{-1}$ h^{-1}, yielding polyethylenes with narrow molecular weight distribution. Pre-catalyst **C1** produced polyethylenes with high molecular weight of up to 10^6 g mol^{-1} and exhibited good thermal stability at elevated reaction temperatures of 60ºC – 80ºC, simultaneously retaining significant catalytic activity.

Experimental section

General consideration

All manipulations involving air- and moisture-sensitive compounds were carried out under nitrogen atmosphere using standard Schlenk techniques. Toluene was refluxed over sodium and distilled under nitrogen prior to use. Methylaluminoxane (MAO, 1.46 M solution in toluene) and modified methylaluminoxane (MMAO, 1.93 M in heptane) were purchased

from Akzo Nobel Corp. Diethylaluminium chloride (Et_2AlCl, 1.17 M in toluene) and dimethylaluminium chloride (Me_2AlCl, 1.00 M in toluene) were purchased from Acros Chemicals. Ethylaluminum sesquichloride (EASC, 0.87 M in toluene) was purchased from Acros Chemicals. High-purity ethylene was purchased from Beijing Yansan Petrochemical Co. and used as received. Other reagents were purchased from Aldrich, Acros, or local suppliers. NMR spectra were recorded on a Bruker DMX 400 MHz instrument at ambient temperature using TMS as an internal standard; IR spectra were recorded on a Perkin-Elmer System 2000 FT-IR spectrometer. Elemental analysis was carried out using a Flash EA 1112 micro-analyzer. Molecular weight and molecular weight distribution (MWD) of polyethylenes were determined by PL-GPC220 at 150ºC, with 1,2,4-trichlorobenzene as the solvent. The melting points of polyethylenes were measured from the second scanning run on a Perkin-Elmer TA-Q2000 differential scanning calorimetry (DSC) analyzer under a nitrogen atmosphere. In the procedure, a sample of about 4.0 mg was heated to 140ºC at a rate of 20ºC/min and kept for 2 min at 140ºC to remove the thermal history and then cooled at a rate of 20ºC/min to −40ºC. ^{13}C NMR spectra of the polyethylenes were recorded on a Bruker DMX 300 MHz instrument at 135ºC in deuterated 1,2-dichlorobenzene with TMS as an internal standard.

Synthesis of the Ligands L1-L6

Acenaphthylene-1,2-bis[2-(bis(4-fluorophenyl)methyl)-4,6-dimethylphenylimine] (**L1**). A mixture of acenaphthylen-1,2-dione (0.364 g, 2 mmol) and 2-[bis(4-fluorophenyl)methyl]-4,6-dimethylbenzenamine (1.294 g, 4 mmol) were dissolved in 10 mL EtOH and 100 mL CH_2Cl_2 containing a catalytic amount of *p*-toluenesulfonic acid and stirred for 24 hours at room temperature. The solvent was evaporated at reduced pressure to give the crude product which was chromatographed on aluminum oxide with petroleum ether-ethyl acetate (V : V = 50 : 1) as an eluent. 0.162 g of the product (orange powder) was obtained in 10.2% isolated yield. Mp: 128–130ºC. FT-IR (cm^{-1}): 2914 (w), 1659 (υ (C=N), m), 1632 (υ (C=N), m), 1599 (m), 1502 (s), 1467 (m), 1273 (m), 1221 (s), 1152 (m), 1094 (m), 1013 (m), 923 (m), 828 (s), 776 (s), 724 (s). Anal. Calc for $C_{54}H_{40}F_4N_2$ (792.90): C, 81.80; H, 5.08; N, 3.53%. Found: C, 81.39; H, 4.97; N,3.48%. ^1H NMR ($CDCl_3$, 400 MHz, TMS): δ 7.70 (d, J = 8.4 Hz, 1H), 7.13 (t, J = 7.6 Hz, 1H), 7.04 (s, 1H), 7.01–6.90 (m, 4H), 6.79–6.76 (m, 2H), 6.61 (s, 1H), 6.31 (d, J = 7.2 Hz, 1H), 6.00 (t, J = 7.6 Hz, 2H), 5.64 (s, 1H), 2.33 (s, 3H), 2.25 (s, 3H). ^{13}C NMR ($CDCl_3$, 100MHz, TMS): δ 163.1, 162.6, 161.4, 160.1, 159.0, 146.2, 139.6, 139.0, 137.5, 133.1, 132.5, 131.2, 131.1, 130.9, 130.8, 129.8, 129.5, 128.7, 128.6, 127.8, 127.1, 125.1, 122.5, 115.0, 114.8, 114.2, 114.0, 50.9, 21.2, 17.8.

Acenaphthylene-1-[2-(bis(4-fluorophenyl)methyl)-4,6-dimethylphenylimine]-2-(2,6-dimethylphenylimine) (**L2**). 2-[2-(bis(4-fluorophenyl)methyl)-4,6-dimethylphenylimino] acenaphthylen-1-one (0.487 g, 1.0 mmol) and 2,6-dimethylbenzenamine (0.363 g, 3.0 mmol) were dissolved in 50 mL toluene and refluxed for 10 h with *p*-toluenesulfonic acid as a catalyst using a Dean-Stark trap. The solution was then evaporated at reduced pressure to give residual solids which were chromatographed on aluminum oxide with petroleum ether-ethyl acetate (V : V = 50 : 1) as an eluent. **L2** was obtained as yellow powder (0.216 g, 36.6% isolated yield). Mp: 182–184ºC. FT-IR (cm^{-1}): 2963 (w), 2915 (w), 1669 (υ (C=N), m), 1641 (υ (C=N), m), 1597 (m), 1503 (s), 1465 (m), 1434 (m), 1223 (s), 1156 (m), 1089 (m), 1030 (m), 921 (m), 832 (s), 774 (s). Anal. Calc for $C_{41}H_{32}F_2N_2$ (590.70): C, 83.36; H, 5.46; N, 4.74%. Found: C, 83.05; H, 5.64; N, 4.71%. ^1H NMR ($CDCl_3$, 400 MHz, TMS): δ 7.84–7.77 (m, 2H), 7.32 (t, J = 7.6 Hz, 1H), 7.20 (t, J = 7.6 Hz, 2H), 7.15 (d, J = 6.8 Hz, 1H), 7.10–7.03 (m, 4H), 7.02–6.89 (m, 4H), 6.64 (s, 1H), 6.60 (d, J = 7.2 Hz, 1H), 6.41 (d, J = 7.2 Hz, 1H), 6.17 (t, J = 8.4 Hz, 2H), 5.70 (s, 1H), 2.33 (s, 3H), 2.26 (s, 3H), 2.09 (s, 3H), 2.07 (s, 3H). ^{13}C NMR ($CDCl_3$, 100MHz, TMS): δ 162.7, 162.5, 162.1, 161.4, 160.3, 159.3, 149.3, 146.4, 140.3, 139.1, 137.9, 133.1, 132.7, 131.4, 131.3, 131.0, 130.6, 129.7, 129.2, 129.1, 128.8, 128.5, 128.4, 128.1, 127.7, 127.6, 125.1, 124.9, 123.9, 122.9, 122.3, 115.1, 114.9, 114.5, 114.3, 51.1, 21.4, 18.3, 17.9, 17.6.

Acenaphthylene-1-[2-(bis(4-fluorophenyl)methyl)-4,6-dimethylphenylimine]-2-(2,6-diethylphenylimine) (**L3**). Using the same procedure as for the synthesis of **L2**, **L3** was obtained as a yellow powder (0.218 g, 35.3% yield). Mp: 130–132ºC. FT-IR (cm^{-1}): 2967 (w), 2932 (w), 1665 (υ (C=N), m), 1644 (υ (C=N), m), 1597 (m), 1504 (s), 1461 (m), 1376 (m), 1220 (s), 1160 (m), 1098 (m), 1039 (m), 925 (m), 824 (s), 775 (s). Anal. Calc for $C_{43}H_{36}F_2N_2$ (618.76): C, 83.47; H, 5.86; N, 4.53%. Found: C, 83.11; H, 5.67; N,4.40%. ^1H NMR ($CDCl_3$, 400 MHz, TMS): δ 7.81–7.76 (m, 2H), 7.30 (t, J = 7.6 Hz, 1H), 7.26–7.23 (m, 4H), 7.19–7.16 (m, 3H), 7.07–7.02 (m, 4H), 6.67 (s, 1H), 6.60 (d, J = 7.2 Hz, 1H), 6.39 (t, J = 7.2 Hz, 1H), 6.19 (t, J = 8.4 Hz, 2H), 5.74 (s, 1H), 2.77–2.68 (m, 1H), 2.63–2.52 (m, 2H), 2.50–2.41 (m, 1H), 2.33 (s, 3H), 2.10 (s, 3H), 1.25 (t, J = 7.6 Hz, 3H), 1.07 (t, J = 7.6 Hz, 3H). ^{13}C NMR ($CDCl_3$, 100MHz, TMS): δ 162.2, 162.5, 161.6, 161.3, 160.2, 159.2, 148.4, 146.4, 140.2, 139.1, 137.8, 137.7, 133.0, 132.7, 131.3, 131.2, 130.9, 130.7, 130.6, 130.4, 129.7, 129.0, 128.9, 128.7, 127.8, 127.6, 127.4, 126.5, 126.4, 126.0, 125.0, 124.1, 122.8, 122.6, 115.0, 114.8, 114.4, 114.2, 50.9, 24.8, 24.6, 21.3, 17.5, 14.5, 13.7

Acenaphthylene-1-[2-(bis(4-fluorophenyl)methyl)-4,6-dimethylphenylimine]-2-(2,6-diisopropylphenylimine) (**L4**). Using the same procedure as for the synthesis of **L2**, **L4** was obtained as a yellow powder (0.229 g, 35.4% yield). Mp: 124–126ºC. FT-IR (cm^{-1}): 2962 (w), 2925 (w), 1674 (υ (C=N), m), 1653 (υ (C=N), m), 1599 (m), 1502 (s), 1462 (m), 1430 (m), 1380 (m), 1216 (s), 1156 (m), 1095 (m), 1042 (m), 922 (m), 823 (s), 775 (s). Anal. Calc for $C_{45}H_{40}F_2N_2$ (646.81): C, 83.56; H, 6.23; N, 4.33%. Found: C, 83.30; H, 6.09; N,4.15%. ^1H NMR ($CDCl_3$, 400 MHz, TMS): δ 7.81–7.76 (m, 2H), 7.31–7.25 (m, 4H), 7.17 (t, J = 7.6 Hz, 1H), 7.06–7.02 (m, 3H), 6.97–6.88 (m, 4H), 6.65 (s, 1H), 6.53 (d, J = 7.2 Hz, 1H), 6.34 (d, J = 7.2 Hz, 1H), 6.16 (t, J = 8.4 Hz, 2H), 5.71 (s, 1H), 3.21–3.14 (m, 1H), 2.94–2.87 (m, 1H), 2.34 (s, 3H), 2.08 (s, 3H), 1.32 (d, J = 6.8 Hz, 3H), 1.20 (d, J = 6.8 Hz, 3H), 1.12 (d, J = 6.8 Hz, 3H), 0.86 (d, J = 6.8 Hz, 3H). ^{13}C NMR ($CDCl_3$, 100MHz, TMS): δ 162.6, 162.5, 161.6, 160.1, 159.1, 147.1, 146.4, 140.2, 139.1, 137.7, 135.5, 135.4, 133.0, 132.6, 131.3, 131.2, 130.9, 130.4, 129.7, 128.9, 128.8, 128.7, 127.6, 127.4, 125.0, 124.5, 123.7, 123.4, 123.0, 122.8, 115.0, 114.8, 114.4, 114.2, 50.9, 28.7, 28.5, 23.9, 23.6, 23.4, 23.1, 21.3, 17.5.

Acenaphthylene-1-[2-(bis(4-fluorophenyl)methyl)-4,6-dimethylphenylimine]-2-(2,4,6-trimethylphenylimine) (**L5**).

Using the same procedure as for the synthesis of **L2**, **L5** was obtained as a yellow powder (0.240 g, 39.7% yield). Mp: 194–196ºC. FT-IR (cm^{-1}): 2968 (w), 2913 (w), 1666 (υ (C=N), m), 1642 (υ (C=N), m), 1598 (m), 1503 (s), 1468 (m), 1431 (m), 1378 (m), 1219 (s), 1156 (m), 1095 (m), 1036 (m), 922 (m), 823 (s), 774 (s). Anal. Calc for $C_{42}H_{34}F_2N_2$ (604.73): C, 83.42; H, 5.67; N, 4.63%. Found: C, 83.20; H, 5.55; N,4.49%. ^{1}H NMR ($CDCl_3$, 400 MHz, TMS): δ 7.83–7.77 (m, 2H), 7.34 (t, J = 7.6 Hz, 1H), 7.20 (t, J = 7.6 Hz, 1H), 7.06–7.01 (m, 4H), 6.96–6.89 (m, 5H), 6.66 (t, J = 7.2 Hz, 2H), 6.41 (d, J = 7.2 Hz, 1H), 6.17 (t, J = 8.8 Hz, 2H), 5.71 (s, 1H), 2.38 (s, 3H), 2.33 (s, 3H), 2.23 (s, 3H), 2.09 (s, 3H), 2.04 (s, 3H). ^{13}C NMR ($CDCl_3$, 100MHz, TMS): δ 162.3, 162.5, 161.6, 161.4, 160.1, 159.2, 146.7, 146.4, 140.1, 139.1, 137.8, 137.7, 133.0, 132.6, 131.3, 131.2, 130.9, 130.4, 129.6, 129.1, 128.9, 128.7, 128.2, 128.0, 127.6, 127.4, 125.1, 124.6, 124.5, 122.8, 122.2, 115.0, 114.8, 114.4, 114.1, 50.9, 21.3, 20.9, 18.1, 17.7, 17.5.

Acenaphthylene-1-[2-(bis(4-fluorophenyl)methyl)-4,6-dimethylphenylimine]-2-(2,6-diethyl-4-methylphenylimine) (**L6**). Using the same procedure as for the synthesis of **L2**, **L6** was obtained as a yellow powder (0.228 g, 36.0% yield). Mp: 116–118ºC. FT-IR (cm^{-1}): 2965 (w), 2925 (w), 1666 (υ (C=N), m), 1643 (υ (C=N), m), 1597 (m), 1502 (s), 1460 (m), 1430 (m), 1375 (m), 1220 (s), 1154 (m), 1094 (m), 1037 (m), 921 (m), 829 (s), 777 (s), 727 (s). Anal. Calc for $C_{44}H_{38}F_2N_2$ (632.78): C, 83.52; H, 6.05; N, 4.43%. Found: C, 83.27; H, 6.09; N,4.50%. ^{1}H NMR ($CDCl_3$, 400 MHz, TMS): δ 7.81–7.76 (m, 2H), 7.32 (t, J = 7.6 Hz, 1H), 7.17 (t, J = 7.6 Hz, 1H), 7.06–7.00 (m, 5H), 6.97–6.89 (m, 4H), 6.65 (s, 2H), 6.36 (d, J = 7.2 Hz, 1H), 6.17 (t, J = 7.2 Hz, 2H), 5.71 (s, 1H), 2.71–2.62 (m, 1H), 2.58–2.49 (m, 2H), 2.43 (s, 3H), 2.33 (s, 3H), 2.37–2.27 (m, 1H), 2.08 (s, 3H), 1.21 (t, J = 7.6 Hz, 3H), 1.04 (t, J = 7.6 Hz, 3H). ^{13}C NMR ($CDCl_3$, 100MHz, TMS): δ 162.6, 162.5, 161.6, 161.5, 160.1, 159.2, 146.4, 145.8, 140.1, 139.1, 137.7, 133.3, 132.9, 132.6, 131.3, 131.2, 130.9, 130.8, 130.5, 130.4, 129.6, 129.0, 128.8, 128.7, 127.8, 127.6, 127.4, 127.3, 127.1, 125.0, 122.8, 122.7, 114.9, 114.7, 114.4, 114.2, 50.9, 24.8, 24.5, 21.3, 21.2, 17.5, 14.6, 13.8.

Synthesis of the Nickel Complexes C1-C6.

The acenaphthylene-1-[2-(bis(4-fluorophenyl)methyl)-4,6-dimethylphenylimino]-2-arylimine (**L1-L6**) were individually reacted with (DME)$NiBr_2$ in dichloromethane to form α-diimine nickel(II) dibromide complexes (**C1-C6**) in good yields. A typical synthetic procedure of **C2** is as follows: Acenaphthylene-1-[2-(bis(4-fluorophenyl)methyl)-4,6-dimethylphenylimine]-2-(2,6-dimethylphenylimine) **L2** (0.124 g, 0.21 mmol) and (DME)$NiBr_2$ (0.062 g, 0.20 mmol) were added to a Schlenk tube together with 10 mL of dichloromethane. After stirring for 24 hours at room temperature, excess diethyl ether was added to precipitate the complex, which was collected by filtration and washed with diethyl ether (3 × 5 mL). Then the collected complex was dried under vacuum to obtain a deep-red powder of **C2** (0.141 g, 87.1%). FT-IR (cm^{-1}): 2973 (w), 2908 (w), 1652 (υ (C=N), w), 1624 (υ (C=N), m), 1601 (m), 1581 (m), 1503 (s), 1465 (m), 1440 (m), 1293 (m), 1222 (s), 1156 (m), 1091 (m), 1043 (w), 827 (s), 774 (s). Anal. Calc for $C_{41}H_{32}F_2N_2NiBr_2$ (809.20): C, 60.85; H, 3.99; N, 3.46%. Found: C, 60.50; H, 3.78; N, 3.13%.

C1 (0.154 g, 76.0% yield.) was obtained as a deep-red powder. FT-IR (cm^{-1}): 2921 (w), 1648 (υ (C=N), w), 1623 (υ (C=N), m), 1601 (m), 1580 (m), 1503 (s), 1468 (m), 1441 (m), 1293 (m), 1221 (s), 1157 (m), 1098 (m), 1042 (m), 831 (s), 774 (s). Anal. Calc for $C_{54}H_{40}F_4N_2NiBr_2$ (1011.40): C, 64.13; H, 3.99; N, 2.77%; found: C, 63.87; H, 3.87; N, 2.84%.

C3 (0.150 g, 89.5% yields.) was obtained as a deep-red powder. FT-IR (cm^{-1}): 2967 (w), 2928 (w), 1653 (υ (C=N), w), 1625 (υ (C=N), m), 1601 (m), 1583 (m), 1504 (s), 1443 (m), 1416 (m), 1295 (m), 1222 (s), 1156 (m), 1094 (m), 1045 (w), 831 (s), 773 (s). Anal. Calc for $C_{43}H_{36}F_2N_2NiBr_2$ (837.26): C, 61.68; H, 4.33; N, 3.35%; found: C, 61.33; H, 4.01; N, 3.11%.

C4 (0.141 g, 81.3% yield.) was obtained as a deep-red powder. FT-IR (cm^{-1}): 2972 (w), 2925 (w), 1654 (υ (C=N), w), 1625 (υ (C=N), m), 1601 (m), 1583 (m), 1504 (s), 1458 (m), 1415 (m), 1295 (m), 1222 (s), 1157 (m), 1130 (m), 1049 (m), 832 (s), 774 (s). Anal. Calc for $C_{45}H_{40}F_2N_2NiBr_2$ (865.31): C, 62.46; H, 4.66; N, 3.24%; found: C, 62.08; H, 4.31; N, 3.15%.

C5 (0.146 g, 88.6% yield.) was obtained as a deep-red powder. FT-IR (cm^{-1}): 2905 (w), 1643 (υ (C=N), w), 1621 (υ (C=N), m), 1599 (m), 1576 (m), 1504 (s), 1440 (m), 1414 (m), 1292 (m), 1224 (s), 1154 (m), 1093 (m), 1048 (m), 830 (s), 774 (s). Anal. Calc for $C_{42}H_{34}F_2N_2NiBr_2$ (823.23): C, 61.28; H, 4.16; N, 3.40%; found: C, 61.08; H, 3.97; N, 3.26%.

C6 (0.152 g, 89.3% yield.) was obtained as a deep-red powder. FT-IR (cm^{-1}): 2963 (w), 2924 (w), 1650 (υ (C=N), w), 1623 (υ (C=N), m), 1600 (m), 1582 (m), 1504 (s), 1457 (m), 1416 (m), 1292 (m), 1222 (s), 1156 (m), 1131 (m), 1045 (m), 829 (s), 776 (s). Anal. Calc for $C_{44}H_{38}F_2N_2NiBr_2$ (851.28): C, 62.08; H, 4.50; N, 3.29%; found: C, 61.77; H, 4.14; N, 3.20%.

X-Ray structure determination

Single-crystal X-ray diffraction study for **C2** and **C5** was conducted on a Rigaku Sealed Tube CCD (Saturn 724+) diffractometer with graphite-monochromated Mo Kα radiation (λ = 0.71073 Å) at 173(2) K, and cell parameters were obtained by global refinement of the positions of all collected reflections. Intensities were corrected for Lorentz and polarization effects and empirical absorption. The structures were solved by direct methods and refined by full-matrix least-squares on F^2. All non-hydrogen atoms were refined anisotropically and all hydrogen atoms were placed in calculated positions. Structural solution and refinement were performed by using the SHELXL-97 package.[13] In the structures of **C2** and **C5**, free solvent molecules which have no influence on the geometry of the main compounds were observed, and the PLATON/SQUEEZE procedure[14] was used to remove these molecules. Crystal data and processing parameters for **C2**, **C5** are summarized in Table **6**.

Table **6**. Crystal data and structure refinement for **C2** and **C5**.

	C2	**C5**
Empirical formula	$C_{41}H_{32}Br_2F_2N_2Ni$	$C_{84}H_{68}Br_4F_4N_4Ni_2$
Fw	809.22	1646.48
T (K)	173 (2)	173 (2)
Wavelength (Å)	0.71073	0.71073
Crystal system	Monoclinic	Monoclinic
Space group	P2(1)/n	P2(1)/c
a (Å)	10.338(2)	19.295(4)

b (Å)	10.828(2)	11.616(2)
C (Å)	32.153(6)	35.044(7)
α (°)	90	90
β (°)	96.32(3)	96.03(3)
γ (°)	90	90
V (Å^3)	3577.3(13)	7811(3)
Z	4	8
D calcd (mg m^{-3})	1.503	1.400
μ (mm^{-1})	2.818	2.583
F (000)	1632	3328
Crystal size (mm)	0.395×0.365×0.194	0.61×0.44×0.09
θ range (°)	1.99-27.45	1.06-27.48
Limiting indices	-13 ≤ h ≤ 13 -14 ≤ k ≤ 14 -41 ≤ l ≤ 41	-25 ≤ h ≤ 24 -14 ≤ k ≤ 14 -27 ≤ l ≤ 45
No. of rflns collected	30438	52967
No. unique rflns [R(int)]	8154 (0.1122)	17699 (0.0760)
Completeness to θ (%)	99.6 %	99.0 %
Absorption correction	Multi-scan	Multi-scan
Data/restraints/params	8145 / 0 / 433	17699 / 0 / 893
Goodness of fit on F^2	1.108	1.061
Final R indices [$I > 2\sigma(I)$]	R1 = 0.0893 wR2 = 0.2192	R1 = 0.0827 wR2 = 0.2077
R indices (all data)	R1 = 0.1051 wR2 = 0.2315	R1 = 0.1234 wR2 = 0.2346
Largest diff peak and hole (e. Å^{-3})	1.655 and -1.192	0.651 and -0.779

Acknowledgements

This work is supported by National Natural Science Foundation of China (NSFC Nos. 21374123 and U1362204). ZF thanks the Chinese Academy of Sciences for the Visiting Scientist Fellowship.

Notes and references

[a] *Key Laboratory of Engineering Plastics and Beijing National Laboratory for Molecular Sciences, Institute of Chemistry, Chinese Academy of Sciences, Beijing 100190, China*

[b] *State Key Laboratory for Oxo Synthesis and Selective Oxidation, Lanzhou Institute of Chemical Physics, Chinese Academy of Sciences, Lanzhou 730000, China*

† Electronic Supplementary Information (ESI) available: CCDC 1042276 and 1042277 contain the supplementary crystallographic data for complexes **C2** and **C5**. These data can be obtained free of charge from The Cambridge Crystallographic Data Centre via www.ccdc.cam.ac.uk/data_request/cif.

1 a) V. C. Gibson, C. Redshaw and G. A. Solan, *Chem. Rev*. 2007, **107**, 1745–1776; b) W.-H. Sun, S. Zhang and W. Zuo, *C. R. Chim*. 2008, **11**, 307–316; c) C. Bianchini, G. Giambastiani, L. Luconi and A. Meli, *Coord. Chem. Rev*. 2010, **254**, 431–455; d) T. Xiao, W. Zhang, J. Lai and W.-H. Sun, *C. R. Chim*. 2011, **14**, 851–855; e) W.-H. Sun, *Adv. Polym. Sci*. 2013, **258**, 163–178; f) R. Gao, W.-H. Sun and C. Redshaw, *Catal. Sci. Technol*. 2013, **3**, 1172–1179; g) S. Wang, W.-H. Sun and C. Redshaw, *J. Organomet. Chem*. 2014**,** **751**, 717–741.

2 a) L. K. Johnson, C. M. Killian and M. Brookhart, *J. Am. Chem. Soc.* 1995, **117**, 6414–6415; b) C. M. Killian, D. J. Tempel, L. K. Johnson and M. Brookhart, *J. Am. Chem. Soc.* 1996, **118**, 11664–11665. c) L. Deng, T. K. Woo, L. Cavallo, P. M. Margl and T. Ziegler, *J. Am. Chem. Soc.* 1997, **119**, 6177–6186. d) D. J. Tempel, L. K. Johnson, R. L. Huff, P. S. White and M. Brookhart, *J. Am. Chem. Soc*. 2000, **122**, 6686–6700.

3 a) T. Xie, K. B. McAuley, J. C. C. Hsu and D. W. Bacon, *Ind. Eng.Chem. Res.* 1994, **33**, 449–479; b) D. P. Gates, S. A. Svejda, E. Onate, C. M. Killian, L. K. Johnson, P. S. White and M. Brookhart, *Macromolecules* 2000, **33**, 2320–2334.

4 a) D. Camacho, E. V. Salo, J. W. Ziller and Z.-B. Guan, *Angew. Chem. Int. Ed.* 2004, **43**, 1821–1825; b) C. Popeney and Z.-B. Guan, *Organometallics* 2005, **24**, 1145–1155; c) J. Liu, D. Chen, H. Wu, Z. Xiao, H.-Y. Gao, F.-M. Zhu and Q. Wu, *Macromolecules*, 2009, **42**, 7789–7796; d) H.-Y. Gao, H. B. Hu, F. M. Zhu and Q. Wu, *Chem. Commun.* 2012, **48**, 3312–3314; e) F.-S. Liu, H.-B. Hu, Y. Hu, L.-H. Guo, S.-B. Zai, K.-M. Song, H.-Y. Gao, L. Zhang, F.-M. Zhu and Q. Wu, *Macromolecules*, 2014, **47**, 3325–3331.

5 a) J. Yu, H. Liu, W. Zhang, X. Hao and W.-H. Sun, *Chem. Commun*. 2011, **47**, 3257–3259; b) W. Zhao, J. Yu, S. Song, W. Yang, H. Liu, X. Hao, C. Redshaw and W.-H. Sun, *Polymer* 2012, **53**, 130–137; c) J. Lai, W. Zhao, W. Yang, C. Redshaw, T. Liang, Y. Liu and W.-H. Sun, *Polym. Chem*. 2012, **3**, 787–793; d) X. Cao, F. He, W. Zhao, Z. Cai, X. Hao, T. Shiono, C. Redshaw and W.-H. Sun, *Polymer* 2012, **53**, 1870–1880; e) W-H. Sun, W. Zhao, J. Yu, W. Zhang, X. Hao and C. Redshaw, *Macromol. Chem. Phys*. 2012, **213**, 1266–1273; f) S. Wang, B. Li, T. Liang, C. Redshaw, Y. Li and W.-H. Sun, *Dalton Trans*. 2013, **42**, 9188–9197; g) J. L. Rhinehart, L. A. Brown and B. K. Long, *J. Am. Chem. Soc.* 2013, **135**, 16316–16319.

6 a) H. Liu, W. Zhao, X. Hao, C. Redshaw, W. Huang and W.-H. Sun, *Organometallics* 2011, **30**, 2418–2424; b) H. Liu, W. Zhao, J. Yu, W. Yang, X. Hao, C. Redshaw, L. Chen and W.-H. Sun, *Catal. Sci. Technol.* 2012, **2**, 415–422; c) S. Kong, C.-Y. Guo, W. Yang, L. Wang, W.-H. Sun and R. Glaser, *J. Organomet. Chem*. 2013, **725**, 37–45. d) C. Wen, S. Yuan, Q. Shi, E. Yue, D. Liu and W.-H. Sun, *Organometallics* 2014, **33**, 7223–7231; e) S. Du, S. Kong, Q. Shi, J. Mao, C. Guo, J. Yi, T. Liang and W.-H. Sun, Organometallics 2015, **34**, 582–590; f) J. L. Rhinehart, N. E. Mitchell and B. K. Long, *ACS Catal.* 2014, **4**, 2501−2504; g) L. Fan, S. Du, C.-Y. Guo, X. Hao and W.-H. Sun, *J. Polym. Sci. Part A: Polym. Chem.* 2015, **53**, accepted

7 a) W.-H. Sun, S. Song, B. Li, C. Redshaw, X. Hao, Y. Li and F. Wang, *Dalton Trans*. 2012, **41**, 11999–12010; b) J. Lai, X. Hou, Y. Liu, C. Redshaw and W.-H. Sun, *J. Organomet. Chem*. 2012, **702**, 52–58; c) X. Hou, Z. Cai, X. Chen, L. Wang, C. Redshaw and W.-H. Sun, *Dalton Trans*. 2012, **41**, 1617–1623; d) X. Hou, T. Liang, W.-H. Sun, C. Redshaw and X. Chen, *J. Organomet. Chem*. 2012, **708–709**, 98–105; e) E. Yue, L. Zhang, Q. Xing, X. Cao, X. Hao, C. Redshaw, and W.-H. Sun, *Dalton Trans*. 2014, **43**, 423–431; f) E. Yue, Q. Xing, L. Zhang, Q. Shi, X.-P. Cao, L. Wang, C. Redshaw and W.-H. Sun, *Dalton Trans*. 2014, **43**, 3339–3346.

8 a) D. Jia, W. Zhang, W. Liu, L. Wang, C. Redshaw and W.-H. Sun, *Cata. Sci. Technol*. 2013, **3**, 2737–2745; b) Q. Liu, W. Zhang, D. Jia, X. Hao, C. Redshaw and W.-H. Sun, *Appl. Catal. A: Gen*. 2014, **475**, 195–202.

9 a) D. Guo, L. Han, T. Zhang, W.-H. Sun, T. Li and X. Yang, *Macromol Theory Simul*. 2002, **11**, 1006–1012; b) T. Zhang, D. Guo, S. Jie, W.-H. Sun, T. Li and X. Yang, *J. Polym. Sci., Part A: Polym. Chem*. 2004, **42**, 4765–4774; c) T. Zhang, W.-H. Sun, T. Li and X. Yang, *J. Mol. Catal. A: Chem*. 2004, **218**, 119–124; d) W. Yang, Y. Chen and W.-H. Sun, *Macromol. Chem. Phys.* 2014, **215**, 1810–1817.

10 a) S. A. Svejda and M. Brookhart, *Organometallics* 1999, **18**, 65–74; b) G. J. P. Britovsek, M. Bruce, V. C. Gibson, B. S. Kimberley, P. J. Maddox, S. Mastroianni, S. J. McTavish, C. Redshaw, G. A. Solan, S. Strolmberg, A. J. P. White and D. J. Williams, *J. Am. Chem. Soc.* 1999, **121**, 8728–8740. c) M. Helldörfer, W. Milius and H. G. Alt, *Inorg.Chim. Acta*, 2003, **351**, 34–42; d) G. J. P. Britovsek, S. A. Cohen, V. C. Gibson and M. V. Meurs, *J. Am. Chem. Soc.* 2004, **126**, 10701–10712. e) B. K. Bahuleyan, G. W. Son, D.-W. Park, C.-S. Ha and I. Kim, *J. Polym. Sci., Part A: Polym. Chem*. 2008, **46**, 1066–1082.

11 G. B. Galland, R. F. de Souza, R. S. Mauler and F. F. Nunes, *Macromolecules* 1999, **32**, 1620–1625.

12 W. Krauss and W. Gestrich, *Chem.-Tech.* 1977, **6**, 513–516.
13 G. M. Sheldrick, SHELXTL-97, Program for the Refinement of CrystalStructures; University of Gottingen, Göttingen, Germany, 1997.
14 A. L. Spek , *Acta Crystallogr*. 2009, **D65**, 148.